

Magnetism of mixed quaternary Heusler alloys: $(\text{Ni,T})_2\text{MnSn}$ ($\text{T}=\text{Cu,Pd}$) as a case study

S.K. Bose

Department of Physics, Brock University, St. Catharines, Ontario, Canada, L2S 3A1

J. Kudrnovský and V. Drchal

Institute of Physics, Academy of Sciences of the Czech Republic, CZ-182 21 Praha 8, Czech Republic

I. Turek

Charles University, Faculty of Mathematics and Physics,

Department of Condensed Matter Physics, Ke Karlovu 5, CZ-12116 Prague 2, Czech Republic

(Dated: August 25, 2010)

The electronic properties, exchange interactions, finite-temperature magnetism, and transport properties of random quaternary Heusler Ni_2MnSn alloys doped with Cu- and Pd-atoms are studied theoretically by means of *ab initio* calculations over the entire range of dopant concentrations. While the magnetic moments are only weakly dependent on the alloy composition, the Curie temperatures exhibit strongly non-linear behavior with respect to Cu-doping in contrast with an almost linear concentration dependence in the case of Pd-doping. The present parameter-free theory agrees qualitatively and also reasonably well quantitatively with the available experimental results. An analysis of exchange interactions is provided for a deeper understanding of the problem. The dopant atoms perturb electronic structure close to the Fermi energy only weakly and the residual resistivity thus obeys a simple Nordheim rule. The dominating contribution to the temperature-dependent resistivity is due to thermodynamical fluctuations originating from the spin-disorder, which, according to our calculations, can be described successfully via the disordered local moments model. Results based on this model agree fairly well with the measured values of spin-disorder induced resistivity.

PACS numbers: 71.23.-k, 72.25.Ba, 75.10.Hk, 75.30.Et

I. INTRODUCTION

Heusler alloys were first studied by the German chemist Friedrich Heusler in 1903, starting with the ordered alloy Cu_2MnSn . Because of their interesting physical properties they have been studied intensively in the past as well as more recently.¹ The most widely studied Heusler alloys are those with the formula Ni_2MnZ ($\text{Z}=\text{Sn,Ga,In}$) and Co_2XY ($\text{X}=\text{Mn, Fe}$; $\text{Y}=\text{Al, Si}$). The former group is of interest because of potential technological applications based on their magnetic shape memory effect,² the magnetocaloric effect,³ and the recently observed giant (negative) magnetocaloric effect.⁴ The latter group holds the promise of application in spintronic devices, thanks to their halfmetallicity at room temperature and above, lattice constant matching with the III-V semiconductors, and large bandgaps. Large tunneling magnetoresistance was measured recently in $\text{Co}_2\text{MnSi/Al-O/Co}_2\text{MnSi}$ magnetic tunneling junctions.⁵

Structurally, most Heusler alloys crystallize in two different cubic phases, having either the L_{21} (X_2YZ) or the C_{1b} (XYZ) symmetry. They can be best visualized as being composed of four interpenetrating fcc-sublattices, shifted along the body diagonal in the order X-Y-X-Z or X-Y-E-Z , where E denotes the empty, i.e. unoccupied, sublattice.¹ An important feature of Heusler alloys is the presence of chemical or substitutional disorder. It is often the non-stoichiometric composition with respect to the ideal systems such

as Ni_2MnSn or Ni_2MnSb which interpolates between the L_{21} Heusler and the C_{1b} semi-Heusler alloys.⁶ Examples are the magnetic shape memory alloys of the type $\text{Ni}_2\text{Mn}_{1+x}\text{Sn}_{1-x}$ (Mn-nonstoichiometry), or the $\text{Ni}_{2-x}\text{MnSb}$ (Ni-nonstoichiometry) alloys.

In addition to the chemical disorder due to nonstoichiometry, a native chemical disorder exists even in 'ideal' ordered alloys X_2YZ and XYZ . In particular, halfmetallic Heusler alloys are very susceptible to such native disorder, a typical example being the Co_2MnSi alloy which exists in the B2-like structure due to Mn-Si disorder.

Finally, there are complex quaternary alloys like the semi-Heusler $(\text{Ni,Cu})\text{MnSb}$ alloys^{7,8} and closely related Heusler alloys like $(\text{Ni,Cu})_2\text{MnSn}$ ⁹ or $(\text{Ni,Pd})_2\text{MnSn}$,¹⁰ with disorder on the X-sublattice. The magnetic properties of these alloys are simplified by the fact that the Mn-sublattice is effectively nonrandom (although there can be some magnetic disorder in a certain concentration range).⁷ In addition, Mn-atoms carry essentially all of the system magnetic moment. However, despite these simplifying features the magnetic, thermodynamic, and transport properties of these alloys are not easy to understand. Several factors: disorder on sublattices neighboring the unperturbed Mn-sublattice, varying carrier concentration, the presence of atoms with different degrees of *d*-electron localization and thus different levels of hybridization with Mn-atoms, all contribute to the complexity of the problem. A reasonably successful interpretation of the results of experiments in Refs.[9,10] was pro-

vided by Stearns^{11,12} using a qualitative model. According to this, magnetic behavior of Heusler alloys is controlled by three types of magnetic interactions, namely: (i) interaction between extended *s*-like electrons and localized *d*-electrons mediated by the *sd*-hybridization, (ii) interaction between localized and delocalized (itinerant) *d*-electrons, and (iii) the superexchange mediated by *sp*-element on the Z-sublattice (Sn in the present case). The dominating interaction is that between the localized and itinerant *d*-electrons and as such the value of the Curie temperature T_c of Heusler alloys is essentially controlled by the amount of itinerant *d*-electrons. This, in turn, is related to the localization of the corresponding *d*-orbitals of the X-atoms. All of the above mentioned interactions are naturally present in the first-principles description of magnetism in the framework of the spin density functional theory (DFT). In general, it is very difficult to separate out the individual contributions from the calculated total interactions.

In this work we employ state-of-the-art electronic structure calculations to understand the properties of disordered quaternary Heusler alloys $(\text{Ni,Cu})_2\text{MnSn}$ and $(\text{Ni,Pd})_2\text{MnSn}$. The exchange interactions are computed from the *ab initio* electronic structure, and then used to estimate the T_c using various approximations. Such a program has been carried out in recent years for a number of conventional (ordered) Heusler alloys. Notable are the pioneering work of Kübler¹³ and extensive studies of electronic and magnetic properties of Heusler alloys, including estimates of the Curie temperature, by Kübler,¹⁴ Galanakis,¹⁵ Picozzi,¹⁶ and Sasioglu and Sandratskii.¹⁷ The study of disordered Heusler alloys is, however, much more involved from a theoretical standpoint because of the presence of disorder violating the translational symmetry. Although in some cases, such as the Heusler alloys with *sp*-disorder on the Z-sublattice, it is possible to use conventional band structure methods (the supercell approach),¹⁸ more sophisticated methods, typically using the coherent potential approximation (CPA) implemented within DFT formalism (DF-CPA), need to be employed^{19,20} to treat disorder in general. This is particularly true for systems with general compositions such as the magnetic shape memory alloys or the Heusler alloys in narrow concentration ranges where abrupt changes in physical properties are known to occur (e.g. around the austenite-martensite transition). So far, such studies have been typically limited to the electronic structure and simple magnetic properties, e.g. magnetic moments. The first attempts to study thermodynamical properties (including T_c) of random alloys have appeared^{6,8} only recently. Particularly worth mentioning is the extensive study of the semi-Heusler alloys $(\text{Cu,Ni})\text{MnSb}$ ⁷ comprising the electronic structure, magnetic, thermodynamical, and transport properties of random alloys in the framework of a unified DFT description.⁷

The aim of the present work is to study electronic, magnetic, thermal, and transport properties of two related disordered Heusler quaternary systems based on the

reference alloy Ni_2MnSn , namely the $(\text{Ni,Cu})_2\text{MnSn}$ and the $(\text{Ni,Pd})_2\text{MnSn}$ systems. Both systems have magnetic moments around $4 \mu_B$ over the whole concentration range but dramatically different concentration dependence of their T_c : strongly nonlinear in the former case and almost linear in the latter. The T_c of end-point alloys, namely X_2MnSn , with $\text{X}=\text{Cu}$, Ni , and Pd , have decreasing values in this order. Thus they seem to obey the criterion advanced by Stearns¹¹ for the dependence of T_c on the localization of *d*-electrons of the element X. Localization of the *d*-electrons increases left to right across a transition metal row, and decreases across a column as we go from 3- to 4- and then to 5-*d*. Thus Cu *d*-electrons are more localized than Ni *d*-electrons, which are more localized than Pd *d*-electrons, explaining the differences in T_c of the three systems in the order mentioned above.

Transport properties of Heusler alloys have not been studied extensively. Some measurements of the temperature dependence of resistivity have been carried out.^{21,22} To our knowledge, no theoretical studies of transport in Heusler alloys have appeared so far. We attempt to fill this gap, using a simplified approach.

II. FORMALISM

The electronic structure calculations were performed using the tight-binding linear muffin-tin orbital (TB-LMTO) scheme²³ in the framework of the local density approximation (LDA). The effect of substitutional disorder on the X-sublattice (either Ni-Cu or Ni-Pd) is described by CPA formulated in the framework of the TB-LMTO Green's function method.²⁴ The same atomic sphere radius was used for all the constituent atoms, and lattice constants were taken from experiments.^{9,10} The calculations employed an *s, p, d, f*-basis. For the parameterization of the local density functional the Vosko-Wilk-Nusair exchange-correlation potential²⁵ was used.

The thermodynamical properties of the system are assumed to be given by a classical Heisenberg Hamiltonian,

$$H_{\text{eff}} = - \sum_{i,j} J_{ij} \mathbf{e}_i \cdot \mathbf{e}_j, \quad (1)$$

where i, j are site indices, \mathbf{e}_i is the unit vector pointing along the direction of the local magnetic moment at site i , and J_{ij} is the exchange integral between sites i and j . The exchange integrals, by construction, contain the atom magnetic moments, their positive (negative) values being indicative of ferromagnetic (antiferromagnetic) coupling.

We evaluate exchange integrals in Eq. (1) using a two-step model,^{26,27} where the band energy is equated to the Heisenberg form and then expressed via multiple scattering formalism based on the TB-LMTO-ASA Green's function in terms of the moments directed along \mathbf{e}_i and \mathbf{e}_j . The reference state for this calculation is chosen to be the disordered local moment (DLM) state.²⁸ Such

a choice was recently suggested for the study of semi-Heusler alloys,⁸ as it has some advantages over the conventional choice of the ferromagnetic reference state.²⁶ The DLM state is closer to the state at which the magnetic transition occurs, compared with the state with a global magnetization. There is no preferred magnetic configuration assumed, and there are no induced moments for the DLM state (see recent discussion of the problem of induced moments in the Heisenberg model in Ref.29). The DLM reference state was successfully used recently in the study of magnetic overlayers on non-magnetic substrates.³⁰ Ideally one would hope the resulting magnetic properties to be robust, i.e. (almost) independent of the assumed reference state. In practice, some dependence on the reference state is unavoidable, and in some cases the DLM reference state has been found to provide better estimates of the Curie temperatures.

We determine the Curie temperature corresponding to the effective Heisenberg model in Eq. (1) by making use of the random-phase approximation (RPA). For comparison, we also include results obtained in the framework of the the mean-field approximation (MFA). The RPA-Curie temperatures are known to be close to those obtained from Monte-Carlo simulations.²⁷

We have used interactions up to ~ 4 lattice constants which are found to be sufficient to achieve reasonably converged results. While it is not a problem to include even more distant interactions in the evaluation of the RPA-Curie temperature, problems arise in connection with integration of the inverse lattice Fourier transform of real-space exchange integrals over the Brillouin zone which becomes a rapidly oscillating function for distant shells. As a result, the RPA Curie temperature oscillates as a function of the shell number included in the above mentioned lattice Fourier transform. It should be noted that such problems do not arise for the MFA or while dealing with semi-Heusler alloys,^{7,8} where the exchange integrals are strongly damped in real-space due to their halfmetallicity.⁶ We have adopted the approach proposed in Ref.31 and used in the context of Heusler alloys in Ref.6. It relies on using a set of exponential damping parameters to compute the T_c , thereby reducing the oscillations and finally extrapolating the results to the zero damping case. This approach was successfully applied to the evaluation of the stiffness constant of ferromagnets in real-space, where the problems associated with using only a limited number of shells are even more severe.³¹ The above-mentioned oscillations are even stronger for the ferromagnetic reference state.

Without an external magnetic field, there are essentially three different contributions to the resistivity of magnetic alloys: (i) phonon scattering, (ii) magnetic scattering due to thermodynamical fluctuations, which are largest close to the Curie temperature,³² and (iii) the residual resistivity due to the presence of chemical disorder on the Ni-Cu and Ni-Pd sublattices.

In this study we limit ourselves to the residual resistivity, and also present a simplified treatment of the resistiv-

ity due to magnetic (spin-disorder) scattering. The residual resistivity is determined by the linear-response theory as formulated in the framework of the TB-LMTO-CPA approach using the Kubo-Greenwood formula,³³ i.e., on the same formal footing as used for the determination of the exchange integrals. This approach, formulated for the multi-sublattice case, allows us to include both the substitutional disorder on the Ni-sublattice as well as magnetic disorder on the Mn-sublattice on an equal footing.³⁴ The disorder-induced vertex corrections are included in the formalism.³⁵ The spin disorder is described here in the framework of the DLM, and treated formally as 'substitutional' disorder via CPA. We refer the reader to Ref.24 for details on the implementation of the DLM in the framework of the TB-LMTO formalism.

III. RESULTS AND DISCUSSION

In this section we present results for the electronic, magnetic, and transport properties of $(\text{Ni,T})_2\text{MnSn}$ ($\text{T}=\text{Cu, Pd}$) alloys over a broad range of concentrations and compare our results with available experimental data.

A. Density of states

Fig. 1 shows the calculated local densities of states (LDOSs) of nonmagnetic X_2MnSn ($\text{X}=\text{Cu, Ni, Pd}$) alloys. Several conclusions follow immediately: (i) all DOSs have a pronounced peak at the Fermi energy (E_F), indicating instability against formation of the ferromagnetic state (Stoner criterion). (ii) The dominant contribution to the peaks is from the Mn-LDOS, which suggests that the magnetism is primarily due to the Mn-sublattice. (iii) The height of Mn-LDOS(E_F) (which is \sim total DOS(E_F)) is approximately the same in all cases, indicating similar magnetic moments for all these compounds (see Fig. 3 below). (iv) The increasing bandwidth of the d -states dominating local X-LDOS in the order Cu-Ni-Pd is clearly seen. This is indicative of decreasing localization (increasing itinerancy) of the d -electrons, resulting in decreasing T_c in the same order, according to the model proposed by Stearns.¹¹ (v) The Cu- and Ni-bands are well separated in energy resulting in a strong diagonal disorder, while their bandwidths are approximately the same (weak off-diagonal disorder). On the contrary, Ni- and Pd-bands differ mainly in their widths (off-diagonal disorder). In all cases, however, X-bands are well separated energetically from the Fermi energy so that disorder on the X-sublattice influences states at E_F only weakly. Hence, the residual resistivity (due to chemical disorder) should be in the weak-scattering regime.

The spin-polarized LDOS for Ni_2MnSn , $(\text{Ni}_{50}\text{Cu}_{50})_2\text{MnSn}$, and Cu_2MnSn are shown in Fig. 2 (top panel). The following conclusions can be drawn: (i) Spin-polarized Cu-LDOSs in Cu_2MnSn are

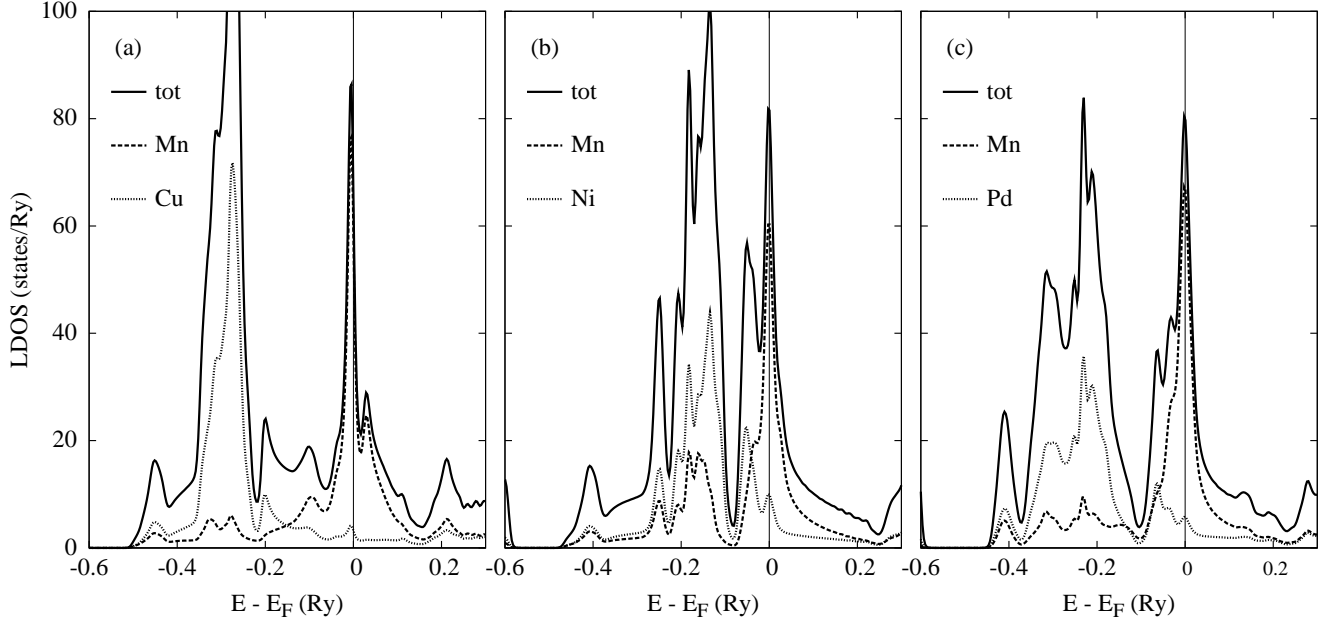


FIG. 1: Total and component resolved densities of states, per formula unit and spin, for nonmagnetic Heusler alloys: (a) ordered Cu_2MnSn , (b) ordered Ni_2MnSn , and (c) ordered Pd_2MnSn .

almost identical, indicating practically no polarization, while some small polarization is seen for corresponding Ni-LDOS in Ni_2MnSn . Similar conclusions are also valid for Cu- and Ni-LDOSs for the equiconcentration case (Fig. 2b). (ii) The total LDOS is smoothed by strong level disorder in the equiconcentration alloy. (iii) Due to large level splitting (large local magnetic moment) the minority Mn-bands in all cases hybridize very little with the X-bands. On the contrary, such hybridization, compared to the nonmagnetic case, is strong for the majority bands even for Cu_2MnSn . (iv) The majority and minority states at the Fermi energy behave differently (corresponding DOSs have different curvature). This results in different Fermi surface geometry for these bands (see e.g. Ref.37). The results for Ni_2MnSn , $(\text{Ni}_{50}, \text{Pd}_{50})_2\text{MnSn}$, and Pd_2MnSn are shown in Fig. 2 (bottom panel). There are some differences in this case: (i) The carrier concentration is the same through the entire alloy system. As a result, the position of the minority Mn-band with respect to the Fermi level stays fixed. This is different from the $(\text{Ni}, \text{Cu})_2\text{MnSn}$ alloy system where the carrier concentration increases with Cu-content. (ii) We observe strong hybridization of Ni- and Pd-bands on the X-sublattice, which differ mostly in their widths. (iii) One thus expects weaker site off-diagonal disorder and, consequently, also lower residual resistivity (see Section III D below).

B. Magnetic moments

Experimental and calculated average moments per formula unit (f.u.) are presented in Fig. 3, together with calculated local moments on Mn-sublattices. There is an overall good agreement between calculated and measured average moments which are essentially concentration-independent and have values around $4 \mu_B$. For the stoichiometric alloys X_2MnSn ($\text{X} = \text{Ni}, \text{Cu}, \text{Pd}$), very similar values were obtained in a previous study by the TB-LMTO-ASA method.³⁶ Mn-sites carry almost all the moment per f.u. and this is particularly true for Cu-rich alloys. Although the calculated magnetic moments agree with experimental values within a few percent, even better agreement can be obtained (e.g. for Ni_2MnSn) when calculations are performed using the generalized gradient approximation (GGA)¹⁷ instead of LDA. The weak concentration dependence of the averaged magnetic moment can be understood from Fig. 2. The large intra-atomic exchange splitting of Mn atoms and the small hybridization of minority Mn-d orbitals with the X-atom orbitals lead to the full occupation of majority Mn-d orbitals, to negligible spin polarization of X- and Sn-atom orbitals, and to composition-independent occupation of minority Mn-d orbitals. These features result in the nearly constant Mn-moment and the total alloy magnetization. The local moments on Ni-sites have values in the range $(0.14, 0.19) \mu_B$ for both systems and all concentrations. The local Cu moments are very small $(0.01-0.02 \mu_B)$, while local Pd-moments are almost concentration-independent, with a value $\sim 0.1 \mu_B$. Finally, local moments on the Sn-

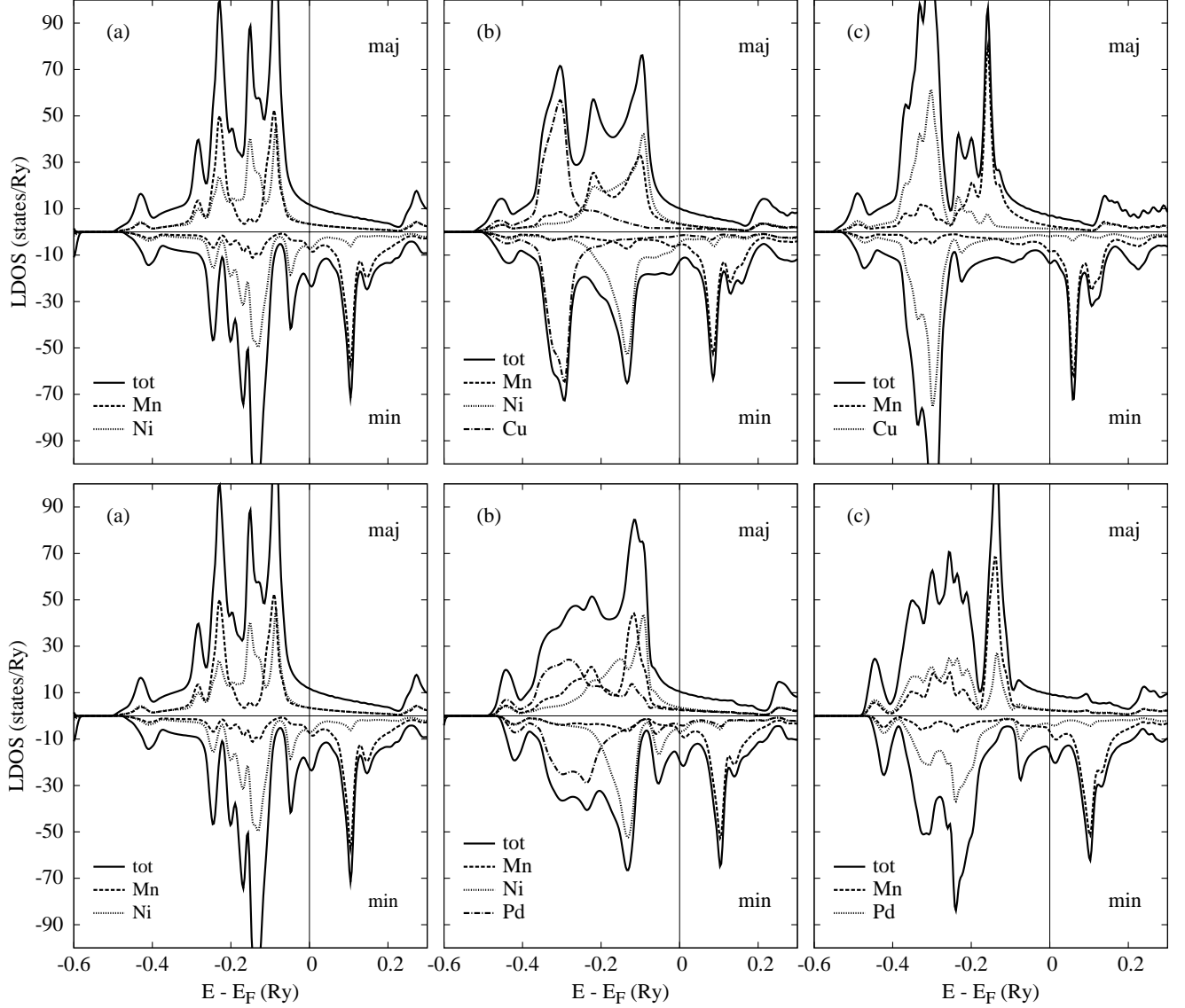


FIG. 2: Total and component resolved densities of states, per formula unit and spin, for ferromagnetic Heusler alloys. Top panel: (a) ordered Ni_2MnSn , (b) disordered $(\text{Ni}_{50},\text{Cu}_{50})_2\text{MnSn}$, and (c) ordered Cu_2MnSn . Bottom panel: (a) ordered Ni_2MnSn , (b) disordered $(\text{Ni}_{50},\text{Pd}_{50})_2\text{MnSn}$, and (c) ordered Pd_2MnSn . Majority (minority) densities of states are shown in upper (lower) parts of each figure.

sublattice are small and negative, in the range $(-0.02, -0.04) \mu_B$.

C. Exchange interactions

1. Calculated results

The exchange integrals are one of the important characteristics of the magnetically polarized state. We have determined them as a function of the alloy composition using the DLM reference state. It should be noted that

for the DLM reference state the only non-zero exchange interactions are those between the Mn sites. The Mn-moments are very rigid and their values in the ferromagnetic and DLM states almost coincide with each other. The leading exchange integrals in $(\text{Ni}_{1-x},\text{Cu}_x)_2\text{MnSn}$ quaternary Heusler alloys are plotted as a function of the Cu-concentration in Fig. 4a. The Mn-sublattice is only indirectly perturbed by the alloy disorder on the X-sublattices, via the hybridization of Ni- and Cu-atoms with the Mn-sublattice. Such a hybridization is weak for Cu-atoms, but strong for the Ni-atoms (see Figs. 1 and 2). In addition to Mn-X hybridization, which varies

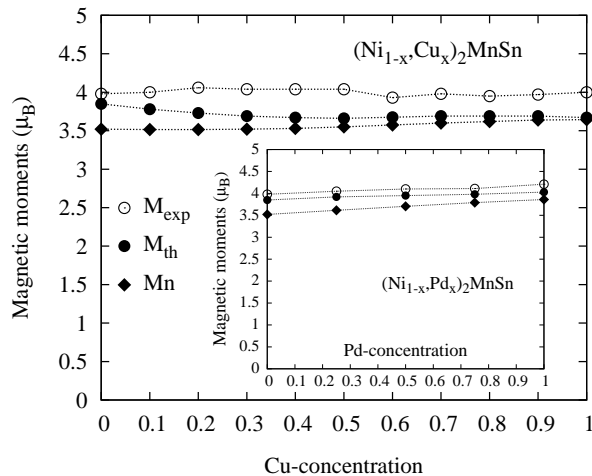


FIG. 3: Averaged magnetic moment (full circle) and local magnetic moments of Mn-atoms (diamonds) as a function of composition for $(\text{Ni,Cu})_2\text{MnSn}$ alloys. Related results for $(\text{Ni,Pd})_2\text{MnSn}$ are shown as inset. Experimental data^{9,10} are denoted by empty circles.

with the alloy composition, there is also an increase of the total electron concentration with the Cu-content due to different valency of Ni- and Cu-atoms. The resulting concentration dependence is quite complex, with the first three exchange integrals being dominant. While the first two are ferromagnetic (FM) and increase with the Cu-content, the third one decreases with Cu-concentration almost linearly and changes its sign from FM to antiferromagnetic (AFM) at about 20% of Cu. It should be noted, however, that the 4th and in particular the 6th neighbor interactions are also non-negligible. To better understand the contribution of the various shells to the magnetic properties we have multiplied the exchange integrals by their degeneracies (N), i.e., by the number of the equivalent atoms in the corresponding shells. This is presented in Fig. 4b. Such terms provide the actual contribution of a given shell to the MFA expression of the Curie temperature.^{26,27} With the multiplication by the degeneracy factors, the contribution of the first shell remains the largest one, and the contributions of the 2nd and 6th shells are suppressed compared to that of the 3rd shell. We have also shown the contribution of the 7th shell, which is non-negligible due to its large degeneracy, even though individual atom contribution is very small.

The above results confirm the assumptions of a theoretical model of Stearns,¹² which asserts that at least three independent magnetic interactions are needed in order to explain the magnetic properties of Heusler alloys with late 3 d and 4 d elements on the X-sublattices. This is a probable cause for the failure of a first-principles study¹³ in which the authors tried to estimate the Curie temperature from just two exchange integrals, based on the energy differences between the FM state and two dif-

ferent AFM states (AF I and AF II with antiparallel alignments of spins along the [100] and [111] directions). A bad estimate of the Curie temperature for such a model for Cu_2MnSn can be attributed particularly to the large contribution of the 3rd shell (see Fig. 4b), which was ignored.

In Fig. 5 we present the results of a similar study for $(\text{Ni}_{1-x}\text{Pd}_x)_2\text{MnSn}$ Heusler alloy. There are some important differences with respect to the $(\text{Ni,Cu})_2\text{MnSn}$ alloy: the number of valence electrons remains unchanged upon alloying, Ni and Pd being neighbors in the same column of the Periodic Table. As already mentioned, the effect of disorder is smaller, as it has predominantly off-diagonal character. The leading interactions are FM, but some interactions, e.g. those from the 4th and 6th shells, are AFM (see Fig. 5a). Upon multiplying the exchange integrals by their shell degeneracy (Fig. 5b), the contributions from the 1st and 3rd shell are seen to be dominant, while the contributions from the 2nd, 5th, and 7th shells (FM) and those of 4th and 6th shells (AFM) tend to compensate each other in the MFA sum. The contributions of all shells are either almost concentration-independent or decrease slightly with the Pd-content, resulting in a linear decrease of the Curie temperature with Pd-concentration (see below).

There is a natural question as to how many shells are needed for a reliable estimate of the Curie temperature. We have just seen that the smallness of exchange integral is not a sufficient condition, as it can be offset by a large degeneracy of the shell. We have insured that the weighted sum of exchange integrals as a function of the shell number achieves its saturation value. For halfmetallic alloys with exponentially damped exchange integrals⁶⁻⁸ this condition is fulfilled for a relatively small number of shells. In transition metal alloys with strong level disorder (see e.g. Ref.38) the situation is similar, because the disorder influences the states at the Fermi energy, which are the relevant states dictating the spatial dependence of exchange integrals.²⁷ However, for the Heusler alloys considered here, the effect of disorder at the Fermi energy is not as strong as in halfmetallic alloys. Hence a larger number of shells needs to be included. We illustrate the situation in Fig. 6, where we plot the mean-field Curie temperature for three typical compositions in $(\text{Ni}_{1-x}\text{Cu}_x)_2\text{MnSn}$ alloy. We note that the mean-field value of the Curie temperature is directly proportional to the sum of the exchange interactions.^{26,27} We observe that for the shell distance $d \leq 4a$, where a is the lattice constant, the results are reasonably saturated. We have thus used all neighbors up to $4a$ and applied the extrapolation procedure briefly described in the Introduction.³¹ This procedure is necessary, as the RPA T_c values oscillate more strongly than the MFA values due to the contribution from the neighborhood of the zone center, where the contribution of the distant shells plays an important role. The estimated error of this procedure is a few percent of the absolute value of the Curie temperature.

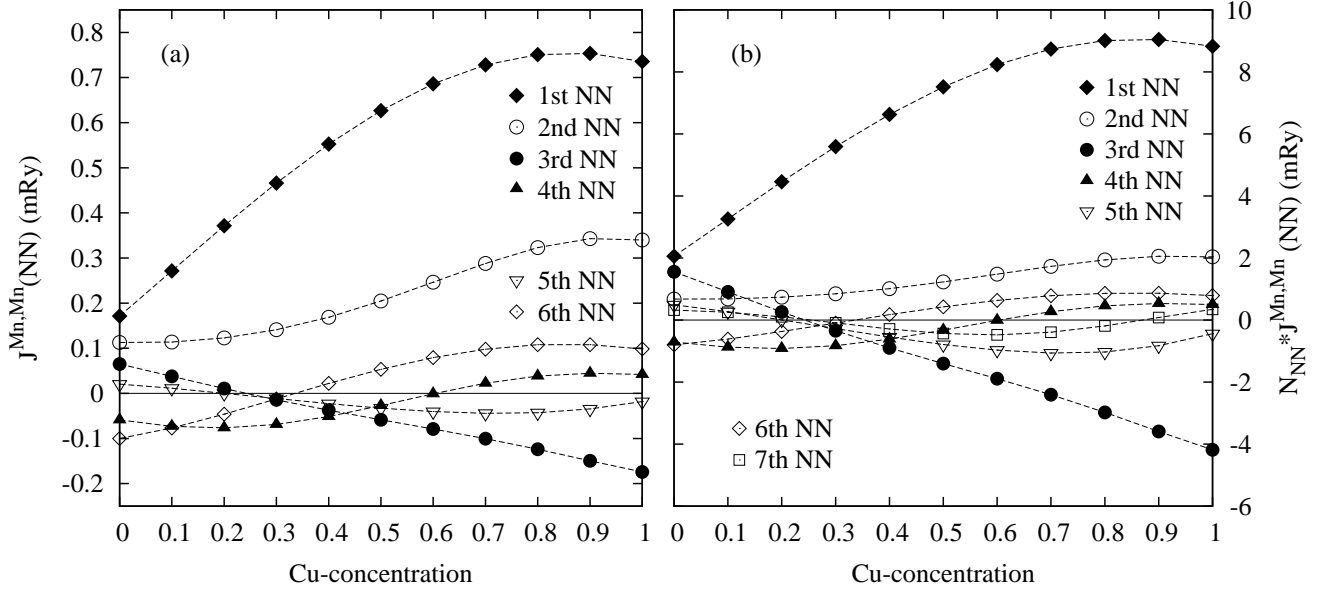


FIG. 4: Concentration dependence of exchange integrals in $(\text{Ni}_{1-x}\text{Cu}_x)_2\text{MnSn}$ Heusler alloys as estimated from the disordered local magnetic reference state: (a) the first six leading (Mn,Mn) -exchange integrals, and (b) the same but with exchange integrals multiplied by their shell degeneracies. We have also added the 7th shell term with a large degeneracy.

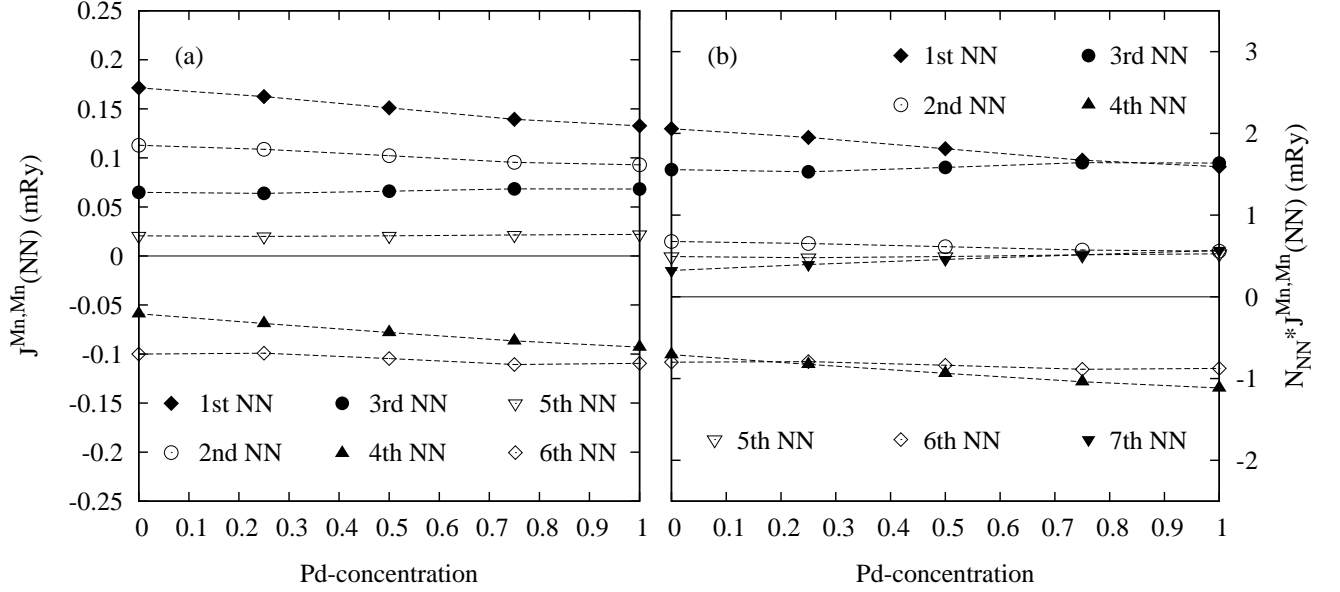


FIG. 5: The same as in Fig. 4 but for $(\text{Ni}_{1-x}\text{Pd}_x)_2\text{MnSn}$ Heusler alloys.

Calculated results for $(\text{Ni,Cu})_2\text{MnSn}$ are presented and compared with experiment⁹ in Fig. 7.

The system $(\text{Ni}_{1-x}\text{Cu}_x)_2\text{MnSn}$ exhibits different behaviors in two concentration regions: for $x \in (0.0, 0.3)$ the Curie temperature stays almost constant with a small minimum at $x \approx 0.3$, while for $x \geq 0.4$ it increases monotonically. Theoretical calculations in the framework of the RPA reproduce the experimental data reasonably

well, both qualitatively and quantitatively. In contrast, the MFA not only overestimates the Curie temperature, but also exhibits a monotonic increase in the whole concentration range, in contrast to the experiment. According to Stearns,¹¹ the larger T_c of Cu_2MnSn compared to that of Ni_2MnSn is due to stronger localization of d -electrons, which enhances the Curie temperature. The flat minimum is explained by the competition of this

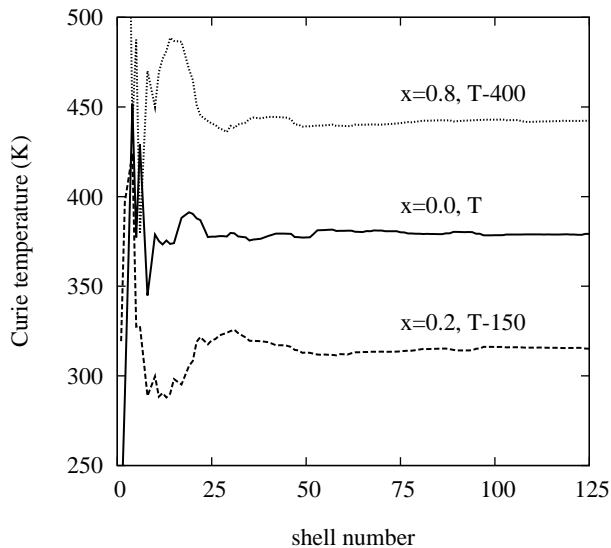


FIG. 6: The mean-field Curie temperature of $(\text{Ni}_{1-x}\text{Cu}_x)_2\text{MnSn}$ for $x=0, 0.2$, and 0.8 illustrating the fulfillment of the saturation of results with respect to the number of shell. Note that curves for $x=0.2$ and 0.8 were shifted to fit the frame.

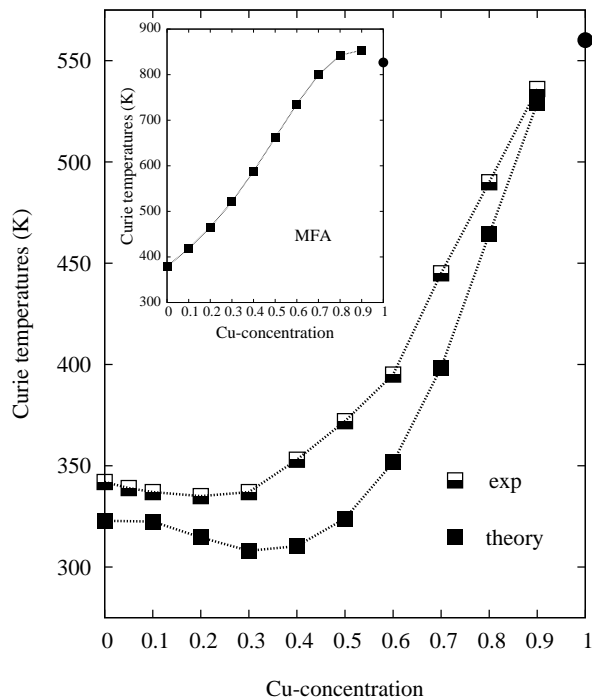


FIG. 7: The concentration dependence of Curie temperatures for $(\text{Ni}_{1-x}\text{Cu}_x)_2\text{MnSn}$. The calculated values (RPA) are compared with experimental data.⁹ The MFA values of Curie temperatures are shown in the inset. Filled circles denote the calculated MFA and RPA Curie temperatures for Cu_2MnSn .

effect with the weakening of this interaction for larger interatomic distances (larger lattice constant) with increasing Cu-content.⁹ It is obvious that this behavior is due to AFM-like exchange interactions of the 3rd shell. For low Cu-concentration this interaction somewhat reduces the RPA sum, and for higher Cu-content its effect is compensated by increasing FM-like interactions.

The calculated Curie temperature for Cu_2MnSn is also shown in Fig. 7. Experimental values are not discussed in Ref.9. There is some controversy in the literature: values 530 K and 630 K can be found, although the lower one is sometimes questioned. The calculated RPA value 560 K lies in the range of the reported experimental values.

The results for Ni_2MnSn alloy can be compared with other theoretical work.³⁹ The experimental values of the Curie temperature range from 328 K to 360 K. The Curie temperature estimated in Ref.39 using the MFA and the FM reference state is 323 K, if only the Mn-Mn exchange integrals are considered. Our related test value is 315 K. The Curie temperature rises to 360 K if Ni-Mn exchange interactions are also included.³⁹ Our mean-field value based on the DLM reference state is 373 K. We would like to point out that good agreement of the Curie temperature obtained in Ref.39 from the FM reference state with the experiment is probably fortuitous, as the RPA would lower this value. The present RPA value based on the DLM reference state (322 K) agrees well with the experiment.

2. Extraction of exchange interactions from experiment

Noda and Ishikawa⁴⁰ have extracted up to 8 nearest-neighbor (NN) exchange interactions for Ni_2MnSn and Pd_2MnSn from the fit to measured inelastic neutron spin-wave scattering data. Taking care of the fact that the authors' exchange integrals do not include spin moments and different definitions of the prefactor in the Heisenberg Hamiltonian, we compare in Fig. 8 our calculated results with the values extracted by Noda and Ishikawa.⁴⁰ The general agreement between the calculated results and the extracted values from the fit appears to be good. It should be noted that calculated exchange integrals are not limited by the distance $2a$ (8 NN) as the fitted ones. In fact, saturation of results with respect to the number of shells is not achieved for 8 NN interactions (see Fig. 5). It is also clear from Table I of Ref.40 that the fitted values can change significantly depending on the number of exchange integrals used for a fit. For example, in case of Ni_2MnSn the 2nd neighbor interaction is larger than that of the 1st neighbor for the 8 NN fit, and smaller for the 6 NN fit.

Ideally, one expects the fitted values to decrease in their sizes. This is not so for a relatively large $J(8)$ in Table I for Ni_2MnSn ⁴⁰ which, for an optimal fit, should be of the smallest magnitude. This indicates that the fitted values should not be taken too literally. Seemingly perfect agreement between the measured magnon spectrum

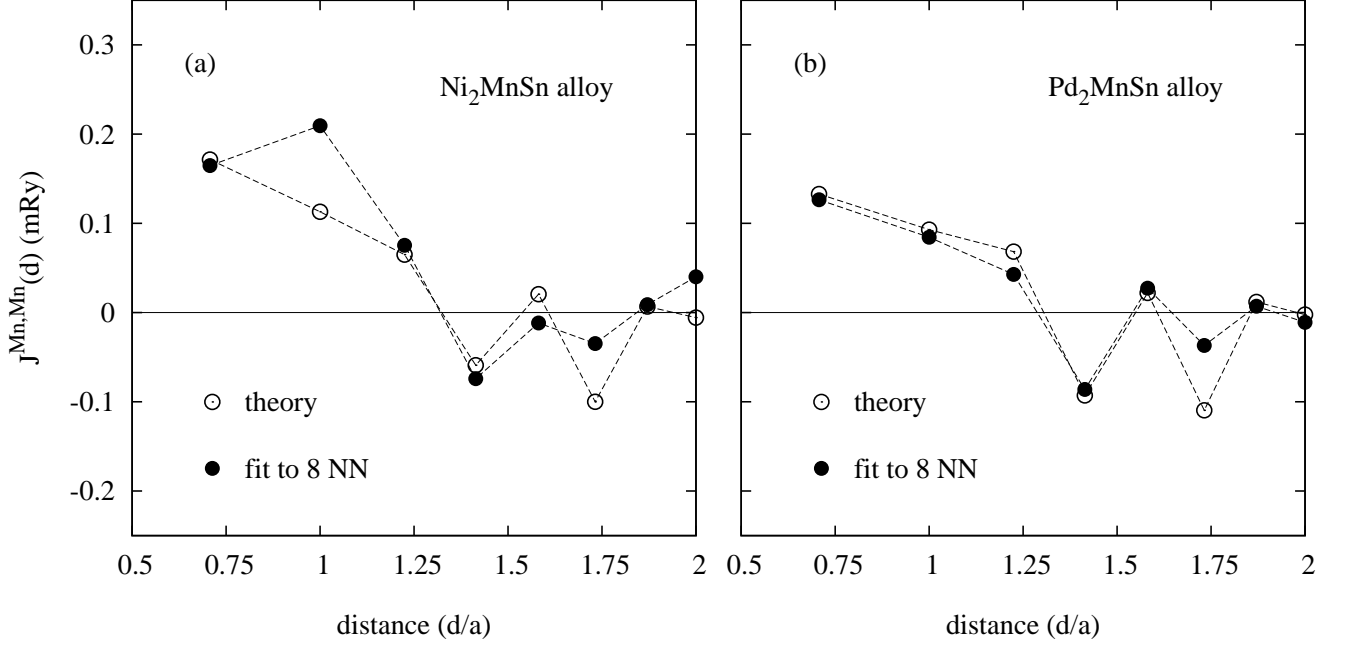


FIG. 8: Comparison of calculated exchange integrals (present paper, theory) with those obtained from the fit to neutron spin-wave scattering experiments (Table I of Ref.40, fit to 8 NN): (a) Ni_2MnSn , and (b) Pd_2MnSn .

and that calculated from the fitted values for Pd_2MnSn in Ref.40 does not guarantee similar agreement in other related magnetic properties.

We also estimate the spin-stiffness constants D_{stiff} for Ni_2MnSn and Pd_2MnSn . The spin-stiffness is a property of the ferromagnetic state, i.e., the state at $T=0$ K. We have therefore estimated D_{stiff} from calculated Mn-Mn exchange integrals in the FM state. The real-space expression for D_{stiff} is non-convergent, and a special treatment is needed for its determination.³¹ Estimated values of D_{stiff} for Ni_2MnSn and Pd_2MnSn are 160 ± 25 (150 ± 10) $\text{meV} \cdot \text{\AA}^2$ and 130 ± 25 (98 ± 10) $\text{meV} \cdot \text{\AA}^2$, respectively. The values in brackets are experimental values,⁴⁰ and the agreement between the theory and experiment is acceptable. The theoretical error bars were estimated from differences in calculated D_{stiff} for various sets of damping constants.³¹

Finally, corresponding results for $(\text{Ni}_{1-x}\text{Pd}_x)_2\text{MnSn}$ alloy are shown in Fig. 9. The experimental values¹⁰ of the Curie temperature lie in the range 190-340 K. In line with the concentration dependence of the exchange integrals (see Fig. 5) one expects a linear decrease of the Curie temperature with the Pd-content. The calculated RPA results show an almost linear decrease of the Curie temperature found in the experiment, although the decrease is smaller than what is observed experimentally.¹⁰ The MFA values are systematically above the RPA as well as the experimental results, but do show the linear decrease of the Curie temperature. Some disorder in Heusler alloys, even for stoichiometric compound, is

rather frequent. In the case of Pd_2MnSn alloy one can speculate about some disorder between Mn- and Sn-sites, which could reduce the calculated Curie temperature (due to antiparallel alignment of Mn-moments). Such a study would require a generalization of the RPA to random systems, which is beyond the scope of the present article.

D. Resistivity

In general, there is very little known about the resistivity of Heusler alloys, either experimentally or theoretically. In magnetic alloys there are three contributions to the resistivity: a temperature-independent part, residual resistivity due to the alloy disorder and other defects, and two temperature-dependent terms due to electron-phonon and electron-magnon scatterings.

1. Residual resistivity

The residual resistivities are calculated using FM reference state, appropriate for zero temperature. The calculated resistivities for $(\text{Ni}_{1-x}\text{Pd}_x)_2\text{MnSn}$, $T=\text{Cu, Pd}$ are shown in Fig.10. The result, an almost parabolic concentration dependence of residual resistivities (Nordheim rule)⁴¹ for both alloys, is in agreement with our discussion of the character of the disorder at the Fermi energy (see Sec. III A), namely its weakness. Much smaller

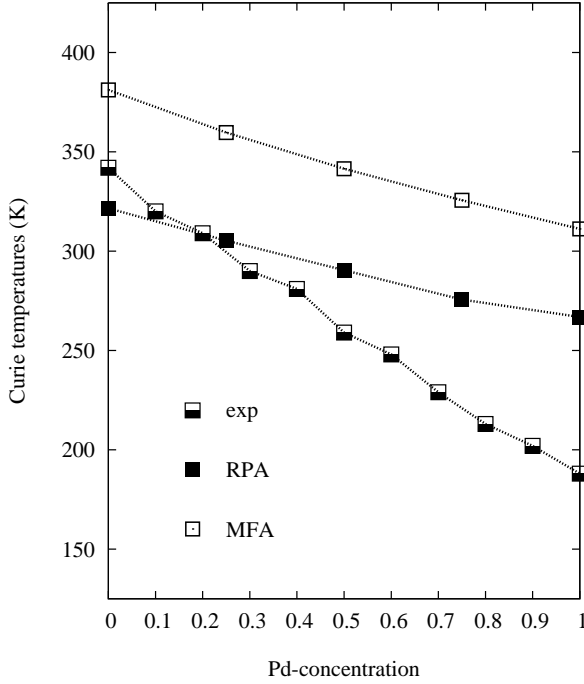


FIG. 9: The same as in Fig. 7 but for $(\text{Ni}_{1-x},\text{Pd}_x)_2\text{MnSn}$. The calculated values (RPA) are compared with experimental data.¹⁰ The MFA values of Curie temperatures are also shown.

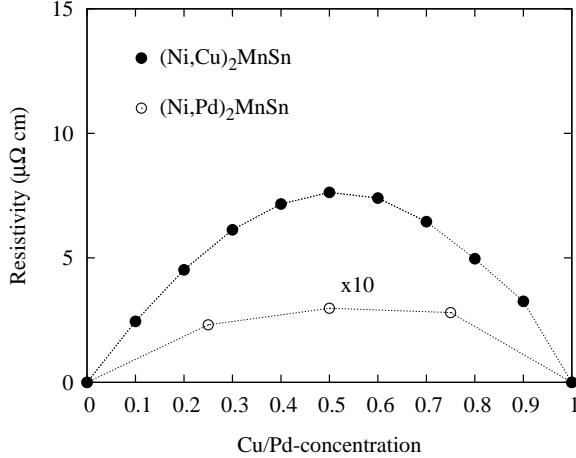


FIG. 10: The concentration dependence of residual resistivities in $(\text{Ni}_{1-x},\text{T}_x)_2\text{MnSn}$ alloys ($\text{T}=\text{Cu}, \text{Pd}$) evaluated for the ferromagnetic ground state at the zero temperature. Note the factor 10 multiplying resistivities for $\text{T}=\text{Pd}$ alloy.

resistivity of $(\text{Ni},\text{Pd})_2\text{MnSn}$ alloy is due to the site off-diagonal disorder, whose effect on the resistivity is weaker than that of the diagonal disorder which dominates in case of $(\text{Ni},\text{Cu})_2\text{MnSn}$.

2. Temperature-dependent resistivity

The contribution due to phonons is relatively well understood,⁴¹ and it is small in Heusler alloys for temperatures around the room temperature.^{21,22} The most important contribution to the temperature-dependent resistivity is due to magnon scattering or the spin-disorder resistivity. A simple theoretical model of the spin-disorder induced resistivity of magnetic alloys was developed some time ago by Kasuya.⁴² This theory explains the experimental facts that for temperatures higher than T_c the resistivity is almost constant, while for temperatures below T_c the resistivity decreases and it is equal to the residual resistivity at zero temperature. The increase of the resistivity with temperature (above $T = 0$ and below T_c) is due to the increasing amount of the spin disorder. The spin-disorder itself is best characterized by the spin-spin correlation function,⁴³ which can be determined from first-principles using known exchange integrals (see e.g. Ref.44). Here we adopt a less ambitious approach. For temperatures above T_c , we assume that a reasonable model of spin-disorder is simply the DLM model, which assumes that the local magnetic moments on atoms are oriented randomly with equal probabilities in all directions. The net moment is zero and the spins are uncorrelated (the spin-spin correlation function is zero in this case). The DLM model is formally equivalent to a random alloy problem,²⁸ and the TB-LMTO-CPA code employing the Kubo Greenwood formula can be used conveniently to compute the resistivity.

Schreiner *et al.*²¹ studied the temperature dependence of resistivity of a series of Heusler alloys including Ni_2MnSn and Pd_2MnSn .²¹ The resistivities calculated for the DLM reference states for $(\text{Ni},\text{T})_2\text{MnSn}$ ($\text{T}=\text{Cu},\text{Pd}$) alloys are presented in Fig. 11. We remind the reader that this resistivity accounts only for the spin-disorder and does not include the part due to scattering from phonons. We observe an increase of the resistivity due to spin-scattering for Cu-impurities in the host Ni_2MnSn and a decrease for Pd impurities. Fig. 11 reflects the decreasing degree of localization (correspondingly, increasing Mn-X hybridization) along the sequence Cu-Ni-Pd, which leads to a decrease of the relative strength of the magnetic disorder, and therefore resistivity, along the same sequence. The corresponding total resistivities measured in the experiment for the ordered Ni_2MnSn and Pd_2MnSn alloys are about $75 \mu\text{Ohm.cm}$ and $50 \mu\text{Ohm.cm}$, respectively. The experimental values obtained after subtraction of the contribution from phonon scatterings are $47 \mu\text{Ohm.cm}$ and $22\text{--}30 \mu\text{Ohm.cm}$. These values compare reasonably well with the values $50 \mu\text{Ohm.cm}$ and $37 \mu\text{Ohm.cm}$ obtained from the present simple theory. In particular, larger value of the spin-disorder induced part of the resistivity in Ni_2MnSn as compared to Pd_2MnSn is correctly reproduced.

We present a simplified treatment of the temperature dependence of resistivity due to spin disorder for temperatures below T_c .^{42,43} We use two simple approaches,

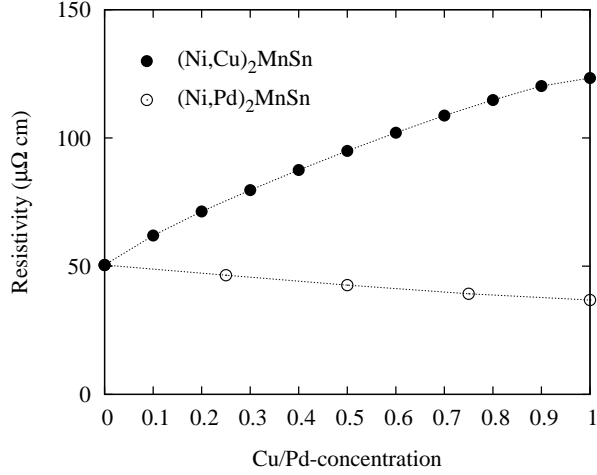


FIG. 11: The concentration dependence of the resistivity of $(\text{Ni}_{1-x}\text{,T}_x)_2\text{MnSn}$ alloys ($\text{T}=\text{Cu, Pd}$) due to the spin-disorder evaluated for temperatures above the Curie temperature. Magnetic state is represented by the disordered local moment (DLM) state.

based on (i) simulation of the temperature dependence through the uncompensated DLM (uDLM) model,^{38,45} and (ii) assuming experimentally observed quadratic temperature dependence of the resistivity due to spin-disorder in combination with calculated values of T_c and the resistivity above the Curie temperature.

The results of the first model are shown in Fig. 12. For a given temperature below T_c we identify the magnetization of the system with that corresponding to the uDLM model with a specific ratio of the parallel and antiparallel spins. We calculate the resistivity for this ratio using the conventional Kubo-Greenwood approach. If there are no antiparallel spins in the system we have the FM state corresponding to the temperature $T=0$ K. On the other hand, for an equal number of parallel and antiparallel spins we have the DLM state with zero total magnetization, corresponding to resistivity at and above the Curie temperature.

Optimally one can determine the magnetization of the system from the present Heisenberg Hamiltonian using statistical mechanical methods. Alternatively, one can adopt some models. We used two, namely the temperature dependence of the magnetization as obtained from the hyperfine field (HF) measurements on Sn atoms in Ni_2MnSn ⁴⁶ and that obtained from similar measurements on Fe-atoms in bcc-Fe.⁴⁷ From the reduced magnetization M/M_0 at a given reduced temperature T/T_c we determine the ratio of parallel and antiparallel spins for the uDLM model, and associate the corresponding reduced resistivity ρ/ρ_c with the reduced temperature T/T_c . For a typical ferromagnetic \leftrightarrow paramagnetic transition the reduced magnetization curve close to $T/T_c=1$ has a universal (system-independent) form. So our results for ρ/ρ_c obtained this way should be more reliable

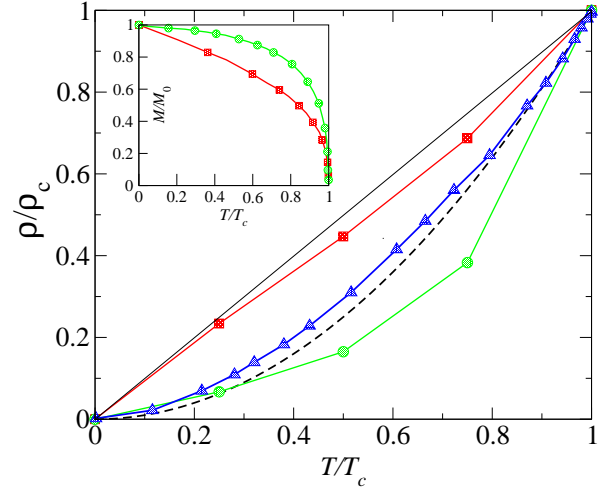


FIG. 12: (Color online) Reduced resistivity $\rho(T)/\rho_c$ vs reduced temperature T/T_c (the suffix c relates to the Curie temperature) for two models of the temperature dependence of the magnetization: (i) as the temperature dependence of the Sn hyperfine field in Ni_2MnSn (squares, Ref.46), and (ii) as the temperature dependence of the Fe hyperfine field in bcc-Fe (circles, Ref.47). The experimental values including the phonon part (triangles) are from Ref.21. The dashed line is a simple quadratic curve, showing the magnon-part of the reduced resistivity. Being in the reduced form, it is actually free of the constant B : $\rho/\rho_c = (T/T_c)^2$. The straight line is used as a guide for eyes. The inset shows the variation of the reduced magnetization M/M_0 as a function of T/T_c determined from Ref.46 (squares) and Ref.47 (circles). M_0 is the saturation magnetization.

in this range. A couple of comments are in order at this point. The HF field at Sn atoms in Ni_2MnSn is not directly proportional to the magnetization. Several models for the dependence of the HF field on the magnetization are discussed in the literature and one such model was used in Ref.46 by Gavriluk *et al.* The seemingly linear decline of magnetization with temperature around $T = 0$ contradicts the Bloch $T^{3/2}$ law, which a typical ferromagnetic material is expected to obey. It is in view of this and the uncertainties involved in relating the HF field at Sn atoms to the magnetization that we include the second model based on bcc Fe as the prototype of a ferromagnetic \leftrightarrow paramagnetic transition. The actual magnetization vs. temperature curve for Ni_2MnSn is expected to lie between the red (squares) and the green (circles) curves shown in the inset of Fig. 12. A typical convex form of the temperature dependence of the reduced resistivity is well reproduced (see Fig. 12) for both cases. The experimental curve including the phonon contribution lies in between these two simple model curves. For comparison, in Fig. 12 we also include the quadratic form $\rho/\rho_c = (T/T_c)^2$ (dashed curve), based on the ex-

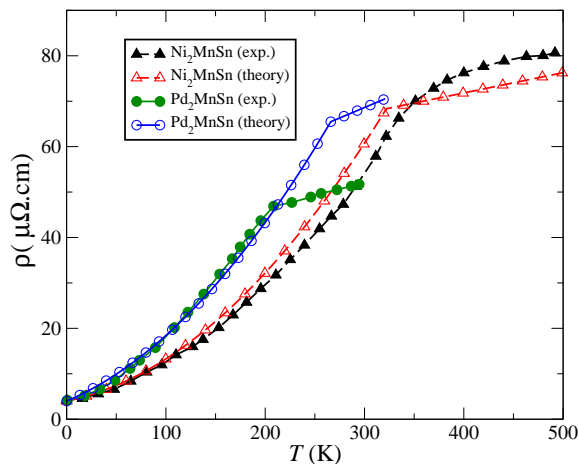


FIG. 13: (Color online) The temperature dependence of the resistivity determined as described in the text for Ni_2MnSn (triangles) and Pd_2MnSn (circles). The empty and full symbols denote the calculated and experimental²¹ results, respectively.

perimental observation that the magnon resistivity has a simple quadratic dependence on temperature.²¹ The difference between the quadratic form (dashed curve) and the experimental curve is the contribution due to the phonons and we see that it is quite small.

In Fig. 13 we display theoretically calculated resistivity assuming the form²¹ $\rho(T) = \rho_0 + AT + BT^2$. The quadratic term is due to the spin disorder,^{42,43} the linear one is the phonon contribution (which is valid with exception of very low temperatures),⁴¹ and ρ_0 is the value of the residual resistivity at $T=0$ K, which is due to all the defects present in the sample. While the values of ρ_0 and the coefficient A were taken from the experiment,²¹ the coefficient B was determined from the calculated T_c and the resistivity in the DLM state. We obtain good agreement between the theory and experiment, in particular for Ni_2MnSn . It should be noted that some offsets of the calculated curves as compared to the experiment are due to differences in calculated and measured T_c which is larger for Pd_2MnSn . Theoretical estimates of the coefficient B are 4.79- and $5.2 \times 10^{-4} \mu\Omega.\text{cm K}^{-2}$ for Ni_2MnSn and Pd_2MnSn , respectively. The corresponding experimental values are 3.94- and $6.1 \times 10^{-4} \mu\Omega.\text{cm K}^{-2}$. Considering the fact that B represents the second derivative of resistivity with respect to temperature, this agreement is good, as evidenced by Fig.13.

IV. CONCLUSIONS

We have studied the electronic, magnetic, thermodynamic, and transport properties of quaternary Heusler

alloys $(\text{Ni,T})_2\text{MnSn}$ ($T=\text{Cu, Pd}$) by means of first-principles density functional method. In agreement with experiments, magnetic moments per formula unit depend only weakly on the alloy composition for both alloys, having values around $4 \mu_B$. Exchange interactions were determined using the DLM reference state, which assumes no *a priori* magnetic ordering in the system. The Curie temperatures were estimated using RPA applied to the non-random Mn-sublattice. The alloy disorder strongly influences values of exchange integrals in $(\text{Ni,Cu})_2\text{MnSn}$ alloys, while only weak concentration dependence of exchange integrals is found for $(\text{Ni,Pd})_2\text{MnSn}$ alloys. Consequently, a linear decrease of the calculated Curie temperature is obtained in the latter alloys in agreement with the experiment. A more complex concentration dependence of exchange integrals in $(\text{Ni,Cu})_2\text{MnSn}$ alloys, in particular different behaviors of Ni-rich and Cu-rich alloys, can be ascribed to the 3rd NN exchange integrals. This result also confirms a model of Stearns¹¹ on the relevance of the first three exchange integrals for magnetic properties of Heusler alloys. In fact, a much larger number of exchange integrals is needed to obtain reasonably stable results in *ab initio* theoretical studies. This is in striking contrast with the related semi-Heusler alloy $(\text{Cu,Ni})\text{MnSb}$,⁷ where the exchange interactions are strongly damped due to their halfmetallicity.

The residual resistivities obey the weak-scattering Nordheim rule. This is due to the fact that strong disorder found e.g. in $(\text{Ni,Cu})_2\text{MnSn}$ alloys influences energy states far from the Fermi energy relevant for electronic transport. Using a simple model for the spin-disorder, we have estimated the temperature dependent resistivity at temperatures above T_c . Reasonably good agreement with experimental results is found for calculations which assume that the resistivity above T_c is essentially captured by the DLM model. Using this value of resistivity and calculated Curie temperatures, good agreement with the experiment was obtained also for the temperature dependence of the resistivity below the Curie temperature.

Acknowledgments

This work was supported by a grant from the Natural Sciences and Engineering Research Council of Canada. J.K. and V.D. acknowledge financial support from AV0Z 10100520 and the Czech Science Foundation (202/09/0775). The work of I.T. has been supported by the Ministry of Education of the Czech Republic (Project No. MSM 0021620834) and by the Czech Science Foundation (Project No. 202/09/0030). J.K. also acknowledges the kind hospitality of the Physics Department at Brock University where most of this work was carried out.

- ¹ P. J. Webster and K. R. A. Ziebeck, "Heusler Alloys," in *Landolt-Börnstein New Series Group III*, Vol. 19C, H. R. J. Wijn (Ed.) (Springer, Berlin, 1988) p. 75.
- ² O. Tegus, E. Brück, L. Zhang, Dagula, K.H. J. Buschow, F.R. de Boer, *Physica B* **319**, 174 (2002).
- ³ K. Ullakko, J.K. Huang, C. Kantner, R.C. OHandley, and V.V. Kokorin, *Appl. Phys. Lett.* **69**, 1966 (1996).
- ⁴ T. Krenke, E. Duman, M. Acet, E.F. Wassermann, X. Moya, L. Mañosa, and A. Planes, *Nature Materials* **4**, 450 (2005).
- ⁵ Y. Sakuraba, M. Hattori, M. Oogane, Y. Ando, H. Kato, A. Sakuma, T. Miyazaki, and H. Kubota, *Appl. Phys. Lett.* **88**, 192508 (2006).
- ⁶ J. Ruzs, L. Bergqvist, J. Kudrnovský, and I. Turek, *Phys. Rev. B* **73**, 214412 (2006).
- ⁷ J. Kudrnovský, V. Drchal, I. Turek, and P. Weinberger, *Phys. Rev. B* **78** 054441 (2008).
- ⁸ B. Alling, A.V. Ruban, and I.A. Abrikosov, *Phys. Rev. B* **79**, 134417 (2009).
- ⁹ E. Uhl, *Monatshefte für Chemie* **113**, 275 (1982).
- ¹⁰ E. Uhl, *Solid State Commun.* **53**, 395 (1985).
- ¹¹ M.B. Stearns, *J. Appl. Phys.* **50**, 2060 (1979).
- ¹² J.R. Reitz and M.B. Stearns, *J. Appl. Phys.* **50**, 2066 (1979).
- ¹³ J. Kübler, A.R. Williams, and C.B. Sommers, *Phys. Rev. B* **28**, 1745 (1983).
- ¹⁴ J. Kübler, *Phys. Rev. B* **67**, 220403(R) (2003).
- ¹⁵ I. Galanakis and Ph. Mavropoulos, *J. Phys.: Condens. Matter* **19**, 315213 (2007) and references there.
- ¹⁶ S. Picozzi, in *First-Principles Study of Ferromagnetic Heusler Alloys: An Overview*, *Advances in Solid State Physics*, vol. **47**, 139 (2008) (Springer).
- ¹⁷ E. Sasioglu, L.M. Sandratskii, and P. Bruno, *Phys. Rev. B* **70**, 024427 (2004).
- ¹⁸ B. Balke, G.H. Fecher, H.C. Kandpal, C. Felser, K. Kobayashi, E. Ikenaga, J.J. Kim, and S. Ueda, *Phys. Rev. B* **74**, 104405 (2006).
- ¹⁹ Y. Miura, K. Nagao, and M. Shirai, *Phys. Rev. B* **69**, 144413 (2004).
- ²⁰ I. Galanakis, K. Özdoğan, B. Aktas, and E. Sasoglu, *Appl. Phys. Lett.* **89**, 042502 (2006).
- ²¹ W.H. Schreiner, D.E. Brandao, F. Ogiba, and J.V. Kunzler, *J. Phys. Chem. Solids* **43**, 1071 (1982).
- ²² G.L. Fraga, J.V. Kunzler, and D.E. Brandao, *J. Phys. Chem. Solids* **46**, 1071 (1985).
- ²³ O.K. Andersen and O. Jepsen, *Phys. Rev. Lett.* **53**, 2571 (1984).
- ²⁴ I. Turek, V. Drchal, J. Kudrnovský, M. Šob, and P. Weinberger, *Electronic Structure of Disordered Alloys, Surfaces and Interfaces* (Kluwer, Boston, 1997); I. Turek, J. Kudrnovský and V. Drchal, in *Electronic Structure and Physical Properties of Solids*, edited by H. Dreyssé, *Lecture Notes in Physics*, Vol. **535** (Springer, Berlin, 2000), p. 349.
- ²⁵ S.H. Vosko, L. Wilk, and M. Nusair, *Can. J. Phys.* **58**, 1200 (1980).
- ²⁶ A.I. Liechtenstein, M.I. Katsnelson, V.P. Antropov, and V.A. Gubanov, *J. Magn. Magn. Mater.* **67**, 65 (1987).
- ²⁷ I. Turek, J. Kudrnovský, V. Drchal, and P. Bruno, *Philos. Mag.* **86**, 1713 (2006).
- ²⁸ B.L. Gyorffy, A.J. Pindor, J. Staunton, G.M. Stocks, and H. Winter, *J. Phys. F: Metal Phys.* **15**, 1337 (1985).
- ²⁹ L. M. Sandratskii, R. Singer, and E. Sasioglu, *Phys. Rev. B* **76**, 184406 (2007).
- ³⁰ J. Kudrnovský, F. Máca, I. Turek, and J. Redinger, *Phys. Rev. B* **80**, 064405 (2009).
- ³¹ M. Pajda, J. Kudrnovský, I. Turek, V. Drchal, and P. Bruno, *Phys. Rev. B* **64**, 174402 (2001).
- ³² T. Kasuya, *Prog. Theor. Phys.* **16**, 58 (1956).
- ³³ I. Turek, J. Kudrnovský, V. Drchal, L. Szunyogh, and P. Weinberger, *Phys. Rev. B* **65**, 125101 (2002).
- ³⁴ I. Turek, J. Kudrnovský, V. Drchal, and P. Weinberger, *J. Phys.: Condens. Matter* **16**, S5607 (2004).
- ³⁵ K. Carva, I. Turek, J. Kudrnovský, and O. Bengone, *Phys. Rev. B* **73**, 144421 (2006).
- ³⁶ Y. Kurtulus, R. Dronskowski, G.D. Samolyuk, and V.P. Antropov, *Phys. Rev. B* **71**, 014425 (2005).
- ³⁷ S. Isida, H. Asato, E. Iwashima, Y. Kubo, and J. Ishida, *J. Phys. F: Metal Phys.* **11**, 1035 (1981).
- ³⁸ J. Kudrnovský, V. Drchal, and P. Bruno, *Phys. Rev. B* **77**, 224422 (2008).
- ³⁹ E. Sasioglu, L.M. Sandratskii, and P. Bruno, *Phys. Rev. B* **71**, 214412 (2005).
- ⁴⁰ Y. Noda and Y. Ishikawa, *Journal of the Phys. Soc. Japan* **40**, 690 (1976).
- ⁴¹ J.M. Ziman, *Electrons and Phonons*, Oxford (1960).
- ⁴² T. Kasuya, *Prog. Theor. Phys.* **16**, 58 (1956).
- ⁴³ M.E. Fisher and J.S. Langer, *Phys. Rev. Lett.* **20**, 665 (1968).
- ⁴⁴ L. Bergqvist, O. Eriksson, J. Kudrnovský, V. Drchal, A. Bergman, L. Nordström, and I. Turek, *Phys. Rev. B* **72**, 195210 (2005).
- ⁴⁵ H. Akai and P.H. Dederichs, *Phys. Rev. B* **47**, 8739 (1993).
- ⁴⁶ A.G. Gavriliuk, G.N. Stepanov, V.A. Sidorov, and S.M. Irkaev, *J. Appl. Phys.* **79**, 2609 (1999), Fig. 7).
- ⁴⁷ M.A. Kobeissi, *Phys. Rev. B* **24**, 2380 (1981).